

Do observations prove that cosmological neutrinos are thermally distributed?

Alessandro Cuoco

*Dipartimento di Scienze Fisiche, Università di Napoli Federico II, and INFN, Sezione di Napoli,
Complesso Universitario di Monte Sant'Angelo, Via Cintia, I-80126 Napoli, Italy*

Julien Lesgourgues

*LAPTH (CNRS-Université de Savoie), B.P. 110, F-74941 Annecy-le-Vieux Cedex, France,
and INFN, Sezione di Padova, Via Marzolo 8, I-35131 Padova, Italy*

Gianpiero Mangano

*Department of Physics, Syracuse University, Syracuse NY, 13244-1130, USA
and INFN, Sezione di Napoli and Dipartimento di Scienze Fisiche, Università di Napoli Federico II,
Complesso Universitario di Monte Sant'Angelo, Via Cintia, I-80126 Napoli, Italy*

Sergio Pastor

*Instituto de Física Corpuscular (CSIC-Universitat de València),
Ed. Institutos de Investigación, Apdo. 22085, E-46071 Valencia, Spain*

(Dated: February 21, 2005)

It is usually assumed that relic neutrinos possess a Fermi-Dirac distribution, acquired during thermal equilibrium in the Early Universe. However, various mechanisms could introduce strong distortions in this distribution. We perform a Bayesian likelihood analysis including the first moments of the three active neutrino distributions as free parameters, and show that current cosmological observations of light element abundances, Cosmic Microwave Background (CMB) anisotropies and Large Scale Structures (LSS) are compatible with very large deviations from the standard picture. We also calculate the bounds on non-thermal distortions which can be expected from future observations, and stress that CMB and LSS data alone will not be sensitive enough in order to distinguish between non-thermal distortions in the neutrino sector and extra relativistic degrees of freedom. This degeneracy could be removed by additional constraints from primordial nucleosynthesis or independent neutrino mass scale measurements.

PACS numbers: 98.80.Cq, 98.70.Vc, 14.60.Pq

I. INTRODUCTION

The large amount of observations of the Cosmic Microwave Background (CMB) which have been accumulated through forty years, since its discovery till the most recent detailed CMB map provided by the Wilkinson Microwave Anisotropy Probe (WMAP) Collaboration [1], shows that relic photons are distributed according to a black body distribution to an incredibly high accuracy. This fact is indeed one of the main cornerstones of the hot Big Bang model, strongly supporting the idea that our Universe expanded starting from high density and temperature conditions.

It is well known that in this framework we expect the Universe to be also filled by a large amount of neutrinos, with present densities of the order of 10^2 cm^{-3} per flavor. These relic neutrinos decoupled from the electromagnetic plasma quite early in time, when weak interaction rates became slower than the Hubble rate for (photon) temperatures in the range $2 \div 4 \text{ MeV}$, just before Big Bang Nucleosynthesis (BBN) took place. Unfortunately the fact that this Cosmic Neutrino Background (C ν B) has today a very small kinetic energy, of the order of 10^{-4} eV , and that neutrinos only interact via weak interactions, prevents us from any possible direct detec-

tion of this background on the Earth (see *e.g.* [2, 3] for a recent review). Nevertheless, there are several indirect ways to constrain the C ν B by looking at cosmological observables which are influenced either by the fact that neutrinos contribute to the Universe expansion rate at all stages, or also via their interactions with the electromagnetic plasma and baryons before their decoupling. In this respect the most sensitive probe is represented by the values of the light nuclide abundances produced during BBN. Actually, the final yields of Deuterium, ^7Li and in particular of ^4He strongly depend on the number of neutrino species as well as on their distribution in phase space at about 1 MeV when the neutron to proton density ratio freezes. In fact, since neutrinos were in chemical equilibrium with the electromagnetic plasma till this epoch we know by equilibrium thermodynamics that they were distributed according to a Fermi-Dirac function, yet BBN can constrain exotic features like the value of their chemical potential [4, 5, 6]. Furthermore, a detailed analysis carried out by several authors [7, 8] shows that neutrinos benefit to a small extent of the entropy released by electron-positron pairs at their annihilation stage, and that this phenomenon reheat neutrinos in a non-thermal way, introducing a small distortion of the order of few percent which grows with the neutrino comoving momentum.

Summarizing, neutrinos are likely to emerge from the BBN epoch as decoupled species with an equilibrium distribution, a smaller temperature with respect to photons by the approximate factor $(4/11)^{1/3}$, possibly a small chemical potential to temperature ratio $|\xi| \leq 0.1^1$ and finally, tiny momentum dependent non-thermal features.

Once decoupled, neutrinos affect all key cosmological observables which are governed by later stages of the evolution of the Universe only via their coupling with gravity. A well known example is their contribution to the total relativistic energy density, which affects the value of the matter-radiation equality point, which in turn influences the CMB anisotropy spectrum, in particular around the scale of the first acoustic peak. Similarly, their number density and their masses are key parameters in the small scale suppression of the power spectrum of Large Scale Structures (LSS), smaller than l_{nr} , the horizon when neutrinos become non-relativistic [9]

$$l_{nr} \sim 38.5 \left(\frac{1 \text{ eV}}{m_\nu} \right)^{1/2} \omega_m^{-1/2} \text{ Mpc} \quad , \quad (1)$$

where $\omega_m = \Omega_m h^2$, with Ω_m the fraction of the critical density due to matter and h the Hubble constant in units of $100 \text{ km s}^{-1} \text{ Mpc}^{-1}$. Several authors have investigated in details these issues assuming a standard Fermi-Dirac distribution for neutrinos, see *e.g.* [6, 10, 11, 12, 13, 14, 15]. In this paper we consider the possibility that the relic neutrino distribution in phase space may be sensibly different and address the following point: how present (and future) cosmological observations can prove that indeed neutrinos are thermally distributed? The implications of a relic neutrino spectrum significantly different from a Fermi-Dirac distribution have been also considered by several authors. For instance, neutrinos could violate the Pauli exclusion principle and obey Bose-Einstein statistics with important cosmological and astrophysical implications [16, 17]. Non-equilibrium neutrino spectra are also produced in low-reheating scenarios [18, 19, 20], from the decays of massive neutrinos into relativistic products (see for instance [21, 22]) or as the result of active-sterile neutrino oscillations after decoupling (see [23] and references therein). A full list of references can be found in [24].

In order to answer the question raised above, we consider in detail (Section II) a simple model where the out of equilibrium decay of a light scalar produces non-thermal features in the neutrino spectra, although our results are quite general and can be also applied to different scenarios. We describe the current bounds on this model in Section III, both from BBN and CMB+LSS.

The expected sensitivity of future cosmological data can be forecast if a fiducial cosmological model is assumed, as described in Section IV. Finally we report our concluding remarks in Section V.

II. THE PHASE-SPACE DISTRIBUTION OF RELIC NEUTRINOS

As we already said, till temperatures of the order of MeV neutrinos are in chemical equilibrium with the electromagnetic plasma, so that they keep an equilibrium distribution. After weak interaction decoupling and in absence of any other interaction process, the collisionless kinetic equations in a Lemaitre-Friedman-Robertson-Walker universe state that, assuming for simplicity instantaneous decoupling, the neutrino and antineutrino distribution in phase-space is a Fermi-Dirac function. Therefore, in terms of the comoving momentum $y = ka$, with a the scale factor and neutrino temperature T_ν , one has

$$df_{\text{th}}(k, T_\nu) = \frac{1}{\pi^2} T_\nu^3 y^2 f_{\text{th}}(y) dy = \frac{1}{\pi^2} T_\nu^3 y^2 \frac{1}{e^y + 1} dy \quad (2)$$

for each flavor. We assume zero chemical potential in the following. Regardless of the specific case at hand, we can specify the flavor α neutrino distribution $df_\alpha(y)$ by the set of moments $Q_\alpha^{(n)}$

$$Q_\alpha^{(n)} = \frac{1}{\pi^2} \left(\frac{4}{11} \right)^{(3+n)/3} T^{3+n} \int y^{2+n} f_\alpha(y) dy \quad , \quad (3)$$

where T is the photon temperature, and we have defined the $Q_\alpha^{(n)}$ in terms of the standard value of the neutrino temperature in the instantaneous decoupling limit $T_\nu = (4/11)^{1/3} T$. For a Fermi-Dirac distribution all moments can be expressed in terms of the number density $Q_\alpha^{(0)}$ or, equivalently, as functions of the only independent parameter T_ν . The first two moments, namely the neutrino energy density defined during the relativistic regime and their number density, enter all present analyses of cosmological observables. More precisely, it is customary to define the effective number of neutrinos

$$N_{\text{eff}} = \frac{120}{7\pi^2} \left(\frac{11}{4} \right)^{4/3} T^{-4} \sum_\alpha Q_\alpha^{(1)} \quad , \quad (4)$$

where $N_{\text{eff}} = 3$ for a thermal distribution, while it gives $N_{\text{eff}} = 3.04$ when including the small effect of neutrino heating during the $e^+ - e^-$ annihilation phase [8]. Similarly, $Q_\alpha^{(0)}$ are related to the present neutrino energy density normalized to the critical density today

$$\omega_\nu = \Omega_\nu h^2 = 0.058 \frac{m_0}{\text{eV}} \frac{11}{4} T^{-3} Q_\alpha^{(0)} \quad , \quad (5)$$

where m_0 is the sum of the neutrino masses and we have assumed for simplicity that the three neutrinos share the

¹ We point out that the bound on ξ is shared by all neutrino species due to flavor oscillations [4], and that a much looser bound is obtained if we allow for extra relativistic degrees of freedom contributing to the Hubble rate during the BBN epoch (see *e.g.* [5]).

same distribution. This is an excellent approximation due to flavor neutrino oscillations (see e.g. [4]). In the standard case we recover the usual result

$$\omega_\nu = \frac{m_0}{94.1[93.2] \text{ eV}} \quad , \quad (6)$$

where the value between brackets takes into account the entropy release to neutrinos from $e^+ - e^-$ annihilations [8]. Actually, there are more parameters which may affect the LSS power spectrum, such as the individual neutrino masses, but their effect is negligible for a fixed m_0 . We now turn to the main point: how the neutrino distributions may acquire non-thermal shapes after the weak interaction freeze-out. A possible source of such non standard contribution may arise from the decays of unstable massive particles provided

- i) decays take place out of equilibrium, *i.e.* for temperatures smaller than the decaying particle mass M . In fact, if decays take place at equilibrium for $T \sim M$, the resulting neutrino distribution would be still thermal, possibly with a different ratio of neutrino-photon temperatures if the entropy is released in different amounts to neutrinos and photons. Therefore, in this case the effect consists at most in an overall constant factor in neutrino distribution, changing the energy density in relativistic species.

- ii) occur after weak interaction freeze-out.

The simplest scenario which we will be considering in details in the following is the two body decay of a light ($M \leq 1$ MeV) neutral scalar particle Φ whose dynamics is dictated by the following lagrangian density

$$\mathcal{L} = \frac{1}{2} \partial_\mu \Phi \partial^\mu \Phi - \frac{1}{2} M^2 \Phi^2 - \frac{\lambda}{\sqrt{3}} \Phi \sum_\alpha \bar{\nu}_\alpha \nu_\alpha + \mathcal{L}_{\text{int}} \quad , \quad (7)$$

with α the flavor index and we have assumed a flavor independent coupling λ to neutrinos. With \mathcal{L}_{int} we denote the interaction terms of Φ with all other fields except neutrinos and responsible for the thermalization of the Φ quanta at high temperatures. The Φ particles are assumed to decay in out of equilibrium conditions before the photon last scattering epoch, so that the produced neutrino burst directly influences the CMB anisotropy spectrum, as well as the late LSS formation. Different scenarios can be envisaged, as for example the case of unstable neutrinos ν_h decaying into a (pseudo) scalar particle φ and a lighter neutrino ν_l ,

$$\nu_h \rightarrow \varphi \nu_l \quad , \quad (8)$$

or three-body decays. It is worth stressing that the aim of this paper is to show how combining different cosmological observables we can constrain the non-thermal contribution to the neutrino background. Despite of the fact that we will be mainly dealing for definiteness with the out of equilibrium Φ decay case, all our results are

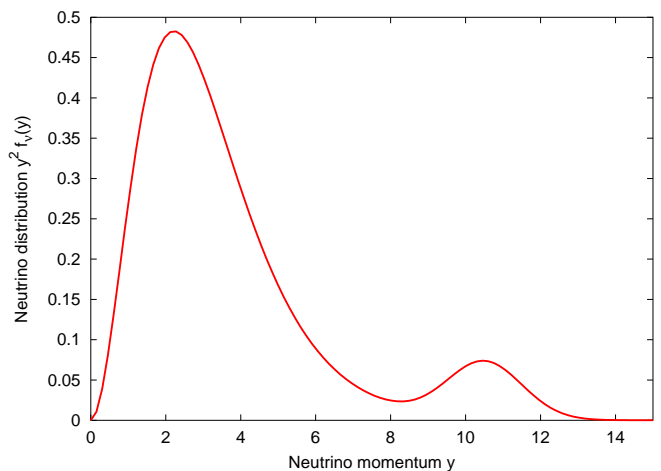


FIG. 1: Differential number density of relic neutrinos as a function of the comoving momentum for the non-thermal spectrum in Equation (11). The parameters are $A = 0.018$, $y_* = 10.5$ and $\sigma = 1$, which corresponds to $N_{\text{eff}} \simeq 4$.

quite general and can be applied to different scenarios as well. Using Eq. (7) we can easily compute the decay rate

$$\Gamma(\Phi \rightarrow \bar{\nu}\nu) = \frac{\lambda^2 M}{8\pi} \quad . \quad (9)$$

If decays take place out of equilibrium for temperatures smaller than the Φ mass it follows that the coupling λ should be very small. In the radiation dominated regime

$$\lambda \sim 10^{-10} \frac{T_D/\text{MeV}}{\sqrt{M/\text{MeV}}} \quad , \quad (10)$$

where T_D is the temperature of the thermal part of the neutrino background at decay. The coupling λ also produces scattering processes like $\Phi\nu \leftrightarrow \Phi\nu$ and crossed reactions, which however receive contribution at order λ^4 . It is easy to see that for the small values implied by Eq. (10) these processes were never in equilibrium before T_D , so they cannot thermalize the Φ particles with neutrinos after decoupling of weak interactions. When the Φ particles decay, the neutrino distribution gets an additional contribution, which in the narrow width limit and in the instantaneous decay approximation at T_D corresponds to a peaked pulse at $y_* = M/(2T_D)$ so that

$$y^2 f(y) dy = y^2 \frac{1}{e^y + 1} dy + \pi^2 \frac{A}{\sqrt{2\pi\sigma^2}} \exp \left[- \left(\frac{y - y_*}{2\sigma^2} \right)^2 \right] \quad , \quad (11)$$

where $\sigma \ll y_*$. Relaxing this assumption would be one of the many ways to generalize our study. We show an example of this non-thermal neutrino spectrum in Figure 1, where a second peak is clearly seen around y_* . With this distribution, and accounting for tiny neutrino heating effects from $e^+ - e^-$ annihilations, the lower moments

expressed in terms of the parameters of Eqs. (4) and (5) read

$$\omega_\nu = \frac{m_0}{93.2 \text{ eV}} \left(1 + 0.99 \frac{2\pi^2}{3\zeta(3)} A \right) , \quad (12)$$

$$N_{\text{eff}} = 3.04 \left(1 + 0.99 \frac{120}{7\pi^2} A y_* \right) . \quad (13)$$

The value of the constant A , which measures the number of neutrinos and antineutrinos produced at decay can be expressed in terms of the total number of Φ particles before decay in a comoving volume

$$A = \frac{2}{3} \frac{n_\Phi}{T_\nu^3} , \quad (14)$$

with n_Φ the Φ number density. Since these particles are decoupled from the thermal bath since at least the BBN epoch, we see that the right hand side of Eq. (14) can be evaluated at this early epoch, so that the largest value of A can be bound by BBN as a function of the Φ mass and number density. We will discuss this issue in the next Section along with the constraints on A and y_* arising from present data on BBN, CMB and LSS. Later we will show in Section IV how future CMB and LSS data could improve these constraints. Our results, which when expressed in terms of the parameters A and y_* get a direct interpretation in the Φ particle decay model described so far, nevertheless can be looked upon as quite general and give the expected sensitivity that future data will likely have in pointing out non-thermal features, if any. This sensitivity, as unfortunately it is quite commonly the case, will be crucially depending on the specific cosmological model which is assumed as a reference one, namely on the number of parameters which enter the data fitting procedure. For example, we will stress that if we enlarge this set of parameters allowing for extra relativistic degrees of freedom in addition to ordinary photons and neutrinos, a parameter degeneracy would make it very difficult to distinguish between non-thermal corrections to the ordinary active neutrino background and the presence of extra exotic light particles.

III. CURRENT BOUNDS FOR A SCENARIO WITH THREE NON-THERMAL NEUTRINOS

A. Constraints from BBN

The amount of light nuclei produced during BBN is rather sensitive to the value of the Hubble parameter H during that epoch, as well as to its time dependence. In particular the ${}^4\text{He}$ mass fraction Y_p strongly depends on the freeze-out temperature of weak processes which keep neutrons and protons in chemical equilibrium. Changing the value of H affects the neutron to proton number density ratio at the onset of the BBN, which is the key parameter entering the final value of Y_p and more weakly the Deuterium abundance. For a fixed baryon density

parameter in the range suggested by results of WMAP, $\omega_b = \Omega_b h^2 = 0.023 \pm 0.001$ [12] both nuclei yields are in fact monotonically increasing functions of H . For recent reviews on BBN see [5, 25, 26]. This fact allows to severely constrain any possible extra contribution to the total energy density due to other species such as the decoupled massive scalar field Φ considered in the present analysis. Defining by T_Φ the corresponding temperature parameter, the energy and number density of Φ particles can be written as

$$\rho_\Phi = \frac{1}{2\pi^2} T_\Phi^4 \int x^2 \left(x^2 + \frac{M^2}{T_\Phi^2} \right)^{1/2} \frac{1}{e^x - 1} dx , \quad (15)$$

$$n_\Phi = \frac{1}{2\pi^2} T_\Phi^3 \int x^2 \frac{1}{e^x - 1} dx = \frac{\zeta(3)}{\pi^2} T_\Phi^3 , \quad (16)$$

where we have assumed, as from our discussion in the previous Section, that the Φ 's decoupled as hot relics well before the onset of BBN. We mention that the effect of massive particles with mass of the order of $1 \div 10$ MeV which are instead coupled to neutrinos or photons during BBN has been studied in details in [27]. The two Eqs. (15) and (16) can be combined getting

$$\rho_\Phi = T_\nu^4 \frac{1}{2\zeta(3)} \left(\frac{n_\Phi}{T_\nu^3} \right) \times \quad (17)$$

$$\int x^2 \left[\left(\frac{\pi^2 n_\Phi}{\zeta(3) T_\nu^3} \right)^{2/3} x^2 + \frac{M^2}{T_\nu^2} \right]^{1/2} \frac{1}{e^x - 1} dx ,$$

so that the upper bound on ρ_Φ from light nuclei abundances translates into an upper limit to n_Φ/T_ν^3 and so to A , see Eq. (14), as a function of M . To get this bound we use a standard likelihood procedure, as discussed *e.g.* in [5], and the BBN numerical code described in details in [25]. We use the WMAP prior on ω_b mentioned before and the experimental result of [28] for D/H

$$\text{D/H} = (2.78_{-0.38}^{+0.44}) \times 10^{-5} . \quad (18)$$

We notice that, allowing for non-thermal features in neutrino distributions may in principle change the preferred value of ω_b and the corresponding uncertainty from a CMB data analysis. However, we will show in the following that the effect on the baryon density parameter is completely negligible and a likelihood analysis provides the same value of a standard ΛCDM model, as considered in [12]. It is therefore consistent to adopt this result in our BBN study.

The ${}^4\text{He}$ mass fraction Y_p obtained by extrapolating to zero the metallicity measurements performed in dwarf irregular and blue compact galaxies is still controversial and possibly affected by systematics. There are two different determinations [29, 30] which are only compatible by invoking the large systematic uncertainty quoted in [29]

$$Y_p = 0.238 \pm (0.002)_{\text{stat}} \pm (0.005)_{\text{sys}} , \quad (19)$$

$$Y_p = 0.2421 \pm (0.0021)_{\text{stat}} . \quad (20)$$

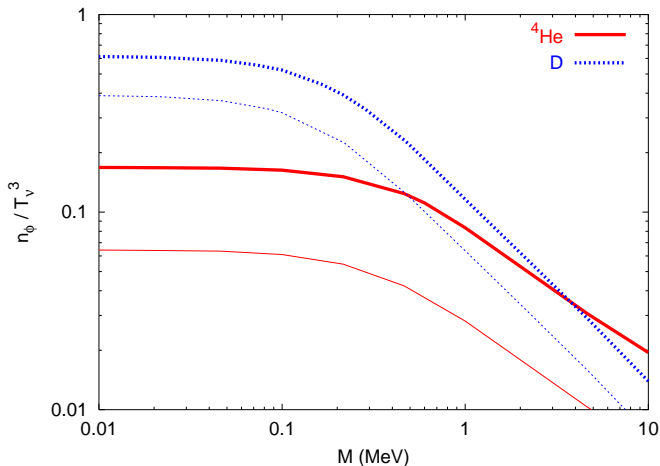


FIG. 2: The 1σ (thin lines) and 2σ (thick lines) BBN bounds on the Φ number density (normalized to T_ν^3) versus mass M in MeV. The regions above the contours would be in disagreement with the observed primordial abundances of ${}^4\text{He}$ or D.

In the present analysis we consider a conservative estimate for the experimental ${}^4\text{He}$ abundance obtained by using the results of [31]

$$Y_p^{\text{exp}} = 0.245 \pm 0.007 . \quad (21)$$

Finally, we do not use the ${}^7\text{Li}$ abundance, since the experimental estimates of this nuclide may be affected by a large depletion mechanism with respect to the primordial value, see *e.g.* [25, 26].

Our results are summarized in Figure 2, where we show the 1σ and 2σ bounds on n_ϕ/T_ν^3 obtained using the ${}^4\text{He}$ mass fraction and D/H, assuming that the Φ 's decay after BBN. As expected the most stringent constraint is due to Y_p , since this parameter is very sensitive to any change of the value of the Hubble parameter. For Φ masses as large as 0.1 MeV, the scalars are relativistic during the neutron to proton density freeze-out, so we get an almost mass independent bound from Y_p of the order of $n_\phi/T_\nu^3 \leq 0.17$ (or $A \leq 0.1$ at 2σ). This corresponds to a limit on the non-thermal component of the neutrino number density of the order 54% of the thermal neutrino contribution. On the other hand, for larger masses the upper bound on n_ϕ/T_ν^3 decreases approximatively as $1/M$ for M larger than few MeV, see Eq. (17). For this mass range, the BBN bound from the D abundance actually becomes slightly more stringent than that from ${}^4\text{He}$. Note that the BBN bounds still allow a large contribution of the decay products to the relativistic neutrino energy density N_{eff} . This value depends quite crucially on the ratio M/T_D , which measures how far from equilibrium conditions the Φ decays take place. For values of M smaller than 0.1 MeV we get

$$N_{\text{eff}} \leq 3.04 \left(1 + 0.1 \frac{M}{T_D} \right) , \quad (22)$$

where $T_D \leq 0.01$ MeV, since we assumed that the Φ decays take place after BBN. If $T_D \sim 0.1M$ or smaller the non-thermal component can give a large or even dominant contribution to N_{eff} . For higher values $M \geq 1$ MeV, our simple scenario becomes unlikely because it requires the Φ decays to take place after BBN, and therefore one needs a very large ratio $M/T_D \geq 10^2$. However, in this case the contribution to N_{eff} can still be very large, despite of the fact that the Φ number density rapidly decreases with increasing values of M . In fact, the upper bound on N_{eff} scales as $1/T_D$ in this regime, see Eq. (13).

B. Adding constraints from cosmological perturbations (CMB and LSS)

We use the public code² CAMB [32] in order to compute the theoretical prediction for the C_l coefficients of the temperature and polarization power spectra of CMB, as well as the matter spectra $P(k)$. We explicitly implement into the code the expression of the non-thermal phase-space distribution function, in the same fashion as massive neutrino chemical potentials were added to CMBFAST [33] in [34]. We focus on three models: the minimal ΛCDM model including three massive neutrinos (with equal mass); our extended model with three non-thermal massive neutrinos ($\Lambda\text{CDM}+\text{NT}$) and finally, for comparison a model with three ordinary massive thermal neutrinos plus extra relativistic degrees of freedom ($\Lambda\text{CDM}+\text{R}$), already analyzed in [11, 35] (using a grid-based method and a smaller dataset). We compute the Bayesian likelihood of each cosmological parameter with a Monte Carlo Markov Chain method, using the public code COSMOMC [36] with option MPI on the MAJORANA cluster at Naples University. The likelihood of each model is found using three groups of data sets, as implemented in the public version of COSMOMC: (i) CMB data: WMAP [12], VSA [37], CBI [38], ACBAR [39]; (ii) LSS data: 32 correlated points from 2dFGRS (up to $k_{\text{max}} = 0.1 h \text{ Mpc}^{-1}$) [40, 41], 14 uncorrelated points from SDSS [42] (up to the same scale); and (iii) SNIa data from Riess et al. [43]. For SDSS, we compare directly the data with the real space linear matter power spectrum multiplied by a scale-independent bias with flat prior, which we marginalize out. For 2dF, we include a prior on the bias: the linear matter power spectrum (at redshift $z = 0$) is rescaled by a redshift-space correction at $z = 0.17$ and a bias factor b

$$P(k)|_{z=0.17}^{\text{red. sp.}} = b^2 \left(1 + \frac{2}{3}\beta_{\text{eff}} + \frac{1}{5}\beta_{\text{eff}}^2 \right) P(k)|_{z=0}^{\text{real sp.}} \quad (23)$$

with $\beta_{\text{eff}} = 0.85\beta$ and $b = \Omega_m^{0.6}/\beta$ (see [44] and references therein). For the redshift-space distortion factor β we adopt the prior $\beta = 0.43 \pm 0.08$ [40]. We do not include

² CAMB Code homepage <http://camb.info/>

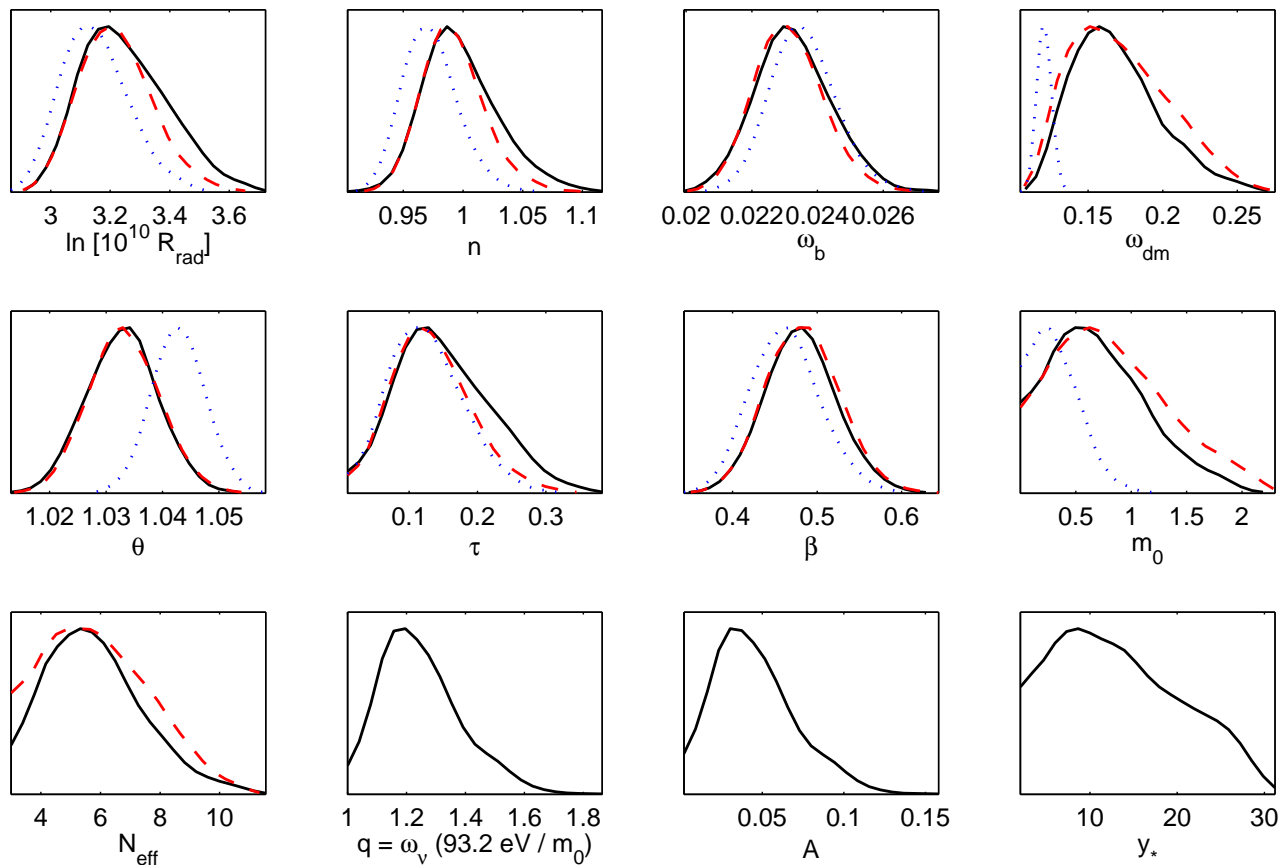


FIG. 3: Marginalized likelihood for the parameters of each model: Λ CDM+NT (black, solid), Λ CDM+R (red, dashed), or Λ CDM (blue, dotted). The independent basis parameters are included in the first ten plots only. The last two plots show the related parameters (A , y_*) for the non-thermal model.

any data from Lyman- α forests³. Finally, we impose the gaussian prior $h = 0.72 \pm 0.08$ (1σ) from the HST Key Project [45], and for the non-thermal model we add the BBN prior described in the previous Section: $A < 0.1$ at the $2\text{-}\sigma$ level (the prior is implemented as a half-gaussian centered at $A = 0$ and with a standard deviation of 0.05). As we already said, a remarkable feature of the Λ CDM+NT model is that BBN does *not* impose an upper limit on N_{eff} at the CMB epoch, so the results shown for comparison in the Λ CDM+R case will *not* include an N_{eff} prior, and will not always be in agreement with

³ The non-thermal model includes massive neutrinos which are individually more energetic and with a higher average momentum than their thermal counterpart. In presence of such a fluid, the non-linear small-scale evolution might differ significantly from that of ordinary Λ CDM models. Therefore, we believe that data from Lyman- α forests are inappropriate for a conservative analysis. We are aware that the bias constraint does rely on observations in the mildly non-linear range $0.2 < k < 0.4 h \text{ Mpc}^{-1}$, and we assume that on these scales the non-thermal neutrinos do not generate unusually large non-linear corrections which would invalidate our bias prior.

predictions from standard BBN. For the Λ CDM model, the basis of cosmological parameters used by the Markov Chain algorithm is as follows: ¹) the overall normalization parameter $\ln[10^{10}\mathcal{R}_{\text{rad}}]$ where \mathcal{R}_{rad} is the curvature perturbation in the radiation era; ²) the primordial spectrum tilt n_s ; ³) the baryon density $\omega_b = \Omega_b h^2$; ⁴) the (cold+hot) dark matter density $\omega_{\text{dm}} = \Omega_{\text{dm}} h^2$; ⁵) θ , the ratio of the sound horizon to the angular diameter distance multiplied by 100; ⁶) the optical depth to reionization τ ; ⁷) the 2dF redshift-space distortion factor β ; ⁸) the total mass m_0 of the three neutrinos. In addition, the Λ CDM+R model includes: ⁹) the effective neutrino number $N_{\text{eff}} = 3.04 + \Delta N_{\text{rel}}$. Finally, the Λ CDM+NT model includes: ⁹) the statistical moment $Q_\alpha^{(1)}$ of the three non-thermal neutrinos, or equivalently, their relativistic energy density in units of that of a standard massless neutrino $N_{\text{eff}} \geq 3.04$, see Eq. (4); ¹⁰) their statistical moment $Q_\alpha^{(0)}$, or equivalently, the dimensionless parameter $q \equiv \omega_\nu(93.2 \text{ eV}/m_0) \geq 1$, see Eqs. (5) and (6). The best value of the effective χ^2 for the three models is shown in the first line of Table I. The Λ CDM+R and Λ CDM+NT do not improve significantly the χ^2 despite of their larger parameter space (for a precise statement

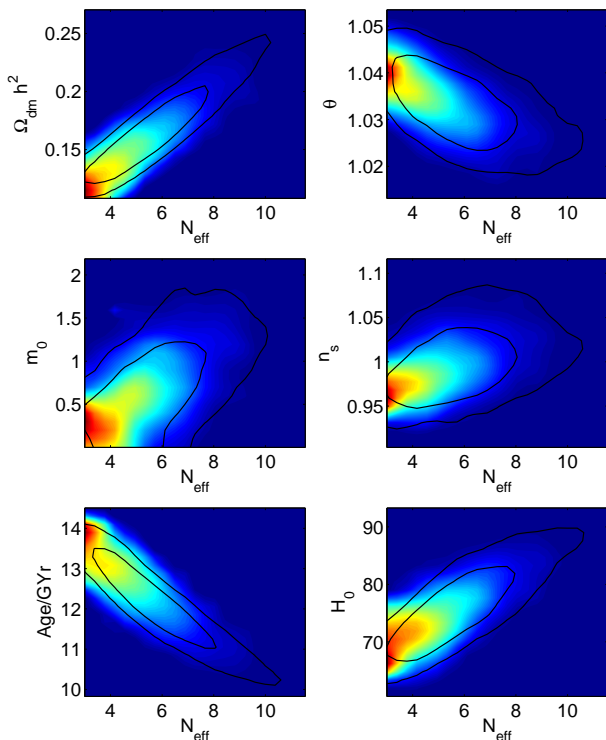


FIG. 4: Two-dimensional likelihoods illustrating the main degeneracy affecting the Λ CDM+NT model (for the Λ CDM+R model the plots are extremely similar). This degeneracy correlates N_{eff} mainly with ω_{dm} (top left) and m_0 (middle left), and to a smaller extent with θ (top right) and n_s (middle right). We also show how N_{eff} is correlated with two related parameters: the age of the Universe (bottom left) and the Hubble parameter (bottom right). The solid curves refer to the $1\text{-}\sigma$ and $2\text{-}\sigma$ contours of the marginalized likelihood. For comparison, the average sample likelihood is shown in color levels.

on the goodness-of-fit of the various models, one should carry a full “evidence” calculation as in [46]). On Figure 3, we plot the marginalized likelihood for each parameter and model. The first ten plots correspond to basis (independent) parameters, while the last two refer to the derived parameters (A , y_*) for the non-thermal case, see Eqs. (12) and (13). The preferred values and $1\text{-}\sigma$ errors for each parameter are shown in Table I.

For the parameters $\ln[10^{10}\mathcal{R}_{\text{rad}}]$, n_s , ω_b , τ , β , the likelihoods are almost equal in the three cases. In particular, the preferred range for the baryon density in the Λ CDM+NT case is still the one of the standard Λ CDM model, as we already anticipated in Section II. On the other hand, in the Λ CDM+R and Λ CDM+NT cases, the θ distribution is significantly shifted, and ω_{dm} and m_0 have much wider error bars. The existence of a degeneracy direction involving mainly ω_{dm} , m_0 and N_{eff} was already pointed out in [11, 35] for the Λ CDM+R model, and is confirmed here for the two models in which the radiation density near the time of decoupling is a free

	Λ CDM	Λ CDM+R	Λ CDM+NT
χ^2_{min}	1688.2	1688.0	1688.0
$\ln[10^{10}\mathcal{R}_{\text{rad}}]$	3.2 ± 0.1	3.2 ± 0.1	3.2 ± 0.1
n_s	0.97 ± 0.02	0.99 ± 0.03	1.00 ± 0.03
ω_b	0.0235 ± 0.0010	0.0231 ± 0.0010	0.0233 ± 0.0011
ω_{dm}	0.121 ± 0.005	0.17 ± 0.03	0.17 ± 0.03
θ	1.043 ± 0.005	1.033 ± 0.006	1.033 ± 0.006
τ	0.13 ± 0.05	0.13 ± 0.06	0.15 ± 0.07
β	0.46 ± 0.04	0.48 ± 0.04	0.48 ± 0.04
m_0 (eV)	0.3 ± 0.2	0.8 ± 0.5	0.7 ± 0.4
N_{eff}	3.04	6 ± 2	6 ± 2
q	1	1	1.25 ± 0.13
h	0.67 ± 0.02	0.76 ± 0.06	0.76 ± 0.05
Age (Gyr)	13.8 ± 0.2	12.1 ± 0.9	12.1 ± 0.8
Ω_Λ	0.68 ± 0.03	0.67 ± 0.03	0.67 ± 0.03
z_{re}	14 ± 4	16 ± 5	18 ± 6
σ_8	0.76 ± 0.06	0.77 ± 0.07	0.77 ± 0.07

TABLE I: Minimum value of the effective χ^2 (defined as $-2\ln\mathcal{L}$, where \mathcal{L} is the likelihood function) and 1σ confidence limits for the parameters of the three models under consideration. The first ten lines correspond to our basis of independent parameters, while the last five refer to related parameters.

parameter⁴. In particular, values as large as $\omega_{\text{dm}} = 0.23$, $m_0 = 1.5$ eV or $N_{\text{eff}} = 9$ are still allowed at the $2\text{-}\sigma$ level by our set of data and priors (while in the standard Λ CDM case we find $\omega_{\text{dm}} < 0.130$ and $m_0 < 0.7$ eV at $2\text{-}\sigma$, in agreement e.g. with [12]). Note however that in the Λ CDM+R case, models with $N_{\text{eff}} > 4$ are in disagreement with standard BBN, while in the Λ CDM+NT case they are not. The degeneracy is illustrated by the two-dimensional likelihood plots of Figure 4. Finally, we can notice that in the Λ CDM+NT model the bound on the parameter $q \equiv \omega_\nu(93.2\text{ eV}/m_0)$ comes essentially from the BBN prior $A < 0.1$, since the CMB and LSS data alone would be compatible with much larger deviations from a thermal phase-space distribution (up to $A = 1$ at $2\text{-}\sigma$). As a final remark we notice that y_* is poorly constrained, and large values for it are still allowed. In the Φ decay scenario this implies that these decays can take place in highly out of equilibrium conditions, $T_D \ll M$, the only bound being instead on the scalar particle number density at the BBN epoch.

⁴ This degeneracy is due to the freedom to increase the total radiation, total matter and critical densities, while keeping fixed the redshift of equality and Ω_Λ . More details can be found in [11].

name	$\ln[10^{10}\mathcal{R}_{\text{rad}}]$	n_s	ω_b	ω_m	Ω_Λ	τ	Y_{He}	b^2	m_0 (eV)	N_{eff}	q
fiducial values	3.1	0.96	0.023	0.14	0.70	0.11	0.24	1.0	0.5	4.0	1.1
1σ error	0.01	0.009	0.0003	0.004	0.02	0.005	0.02	0.08	0.3	0.1	0.7 (conservative)
	0.006	0.003	0.0001	0.0007	0.001	0.003	0.004	0	0.03	0.02	0.08 (ambitious)

TABLE II: Expected errors on the parameters of the Λ CDM+NT model. The first line shows the fiducial values, *i.e.* the parameter values assumed to represent the best fit to the data. The next lines give the associated 1σ errors for the “conservative” and “ambitious” sets of future experiments as described in the text.

IV. FUTURE PROSPECTS: CAN WE REMOVE THE DEGENERACIES?

A. Error forecast assuming no extra relativistic degrees of freedom

We will now compute the error expected from future experiments on the parameters of the Λ CDM+NT model. Of course, the results that will be derived here are model-dependent, since we assume that the cosmological evolution can be described with a given set of cosmological parameters. The issue of generalization to larger classes of models will be considered in the next Section. As usually done in this kind of analysis, we first assume that future data will favor a particular Λ CDM+NT model that we call the “fiducial model”, with cosmological parameter values $x_i = \bar{x}_i$. Then, we compute the Fisher matrix

$$F_{ij} = -\frac{\partial^2 \ln \mathcal{L}}{\partial x_i \partial x_j}(\bar{x}_i) \quad , \quad (24)$$

which represents the curvature of the likelihood distribution \mathcal{L} near its maximum for a given set of future experiments with known sensitivity. Inverting the Fisher matrix, we obtain the $1\text{-}\sigma$ error on each parameter, assuming that all other parameters are unknown

$$\frac{\Delta x_i}{x_i} = (F^{-1})_{ii}^{1/2} \quad . \quad (25)$$

The present analysis follows the lines of that in [47], and we refer the reader to this work for details on the expression of the likelihood distribution, for the description of future experimental sensitivities and for references of seminal papers on the subject. When computing numerically the derivative of the likelihood with respect to each cosmological parameter, we choose the smallest possible step size above the threshold set by the precision of CMBFAST, and we check that the final result is almost independent of the exact step value. Our first “conservative” set of experiments consists in the Planck satellite⁵ (without lensing information [48]) combined with the completed SDSS redshift survey⁶ with effective volume $V_{\text{eff}} = 1 h^{-3} \text{ Gpc}^3$ and a free bias. We

assume that the SDSS data can be compared with the predictions of linear perturbation theory up to the scale $k_{\text{max}} = 0.1 h \text{ Mpc}^{-1}$. The second “ambitious” set consists in CMBPOL⁷ combined with a large survey with effective volume $V_{\text{eff}} = 40 h^{-3} \text{ Gpc}^3$, no bias uncertainty, and $k_{\text{max}} = 0.2 h \text{ Mpc}^{-1}$, which should mimic the properties of a large cosmic shear survey like the LSST project⁸ (this estimate should be regarded as indicative only, since for simplicity we compute the Fisher matrix from the matter power spectrum instead of the spectrum of the projected gravitational potential).

The results are shown in Table II for a fiducial model comfortably allowed by current bounds, with $N_{\text{eff}} = 4$, $q = 1.1$ and $m_0 = 0.5 \text{ eV}$, corresponding to non-thermal correction parameters $A = 0.018$ and $y_* = 10.5$. For this model, the neutrinos enter the non-relativistic regime well after decoupling, and only contribute to 0.5% of the critical density today. As a consequence, the two parameters q and m_0 are measurable only from the free-streaming effect in the matter power spectrum, while all other parameters have a clear signature in the CMB anisotropies. More precisely, a combination of these two parameters (close to $q \times m_0 \propto \omega_\nu$ at first approximation) controls the amplitude of the free-streaming suppression on small scales, while the orthogonal combination controls the details of the transition on intermediate scales. Since LSS experiments do not have enough resolution for constraining this last combination, we expect a large degeneracy between q and m_0 , which is confirmed by the diagonalization of the Fisher matrix. The direction $\Delta q = (\Delta m_0 / 0.5 \text{ eV})$ appears to be poorly constrained. As a consequence, the errors quoted in Table II for m_0 are larger (typically by a factor two) than those expected for thermal neutrinos, and q has the biggest relative error. Notice that we are not applying in this case any prior on q , as was instead the case in the previous Section, where this parameter was related to the Φ number density at the BBN epoch in the Φ to neutrino decay scenario. Therefore, results in Table II are independent of any particular model that produces a distortion on the relic neutrino spectrum.

The remarkable result of this Section is that in spite of this degeneracy, future experiments can provide some insight on non-thermal features and still measure the neu-

⁵ <http://www.rssd.esa.int/index.php?project=PLANCK>

⁶ <http://www.sdss.org>

⁷ <http://universe.nasa.gov/program/inflation.html>

⁸ <http://www.lsst.org>

trino mass with good precision even when the thermal assumption is relaxed. The error for all parameters but (q , m_0) are close to the usual expectations based on thermal neutrinos (see [47] for comparison). A small distortion of the first moment described by $q \sim 1.16$ would be sufficient for a $2\text{-}\sigma$ detection with CMBPOL+LSST. Notice that large distortions (close to the current upper bounds) would lead to smaller errors than those quoted in Table II due to their additional direct effect on the CMB.

B. Degeneracy between non-thermal corrections and extra relativistic degrees of freedom

The bounds derived in the previous Sections depend on the assumption that the cosmological observations can be described within the framework of the Λ CDM+NT model. In the future, we would be in a position to make such an analysis if we had some independent motivations for the introduction of non-thermal distortions in the neutrino background. Otherwise, even if the best-fit Λ CDM+NT model turned out to be much more likely than the best-fit Λ CDM, many alternative models would compete with each other.

The Λ CDM+NT model has a natural “competitor”, which is the previously discussed Λ CDM+R model, with three standard massive neutrinos and extra relativistic degrees of freedom. Indeed, in the two models the amplitude and scale of the free-streaming effect can be tuned independently, which is not usually the case (and which cannot be mimicked by the introduction of tilt running, spatial curvature, tensor modes, isocurvature modes, etc.)

The results of Section III B suggest that at least within current experimental sensitivities, the two models are roughly equivalent. However, many theoretical arguments suggest that the intrinsic differences between the two cases can lead to distinct observable signatures. For instance, the non-thermal corrections boost the average neutrino momentum, so at the level of the equations the free-streaming effect is never strictly identical in the two cases.

We have investigated in more details the issue of a possible (at least approximate) one-to-one correspondence between Λ CDM+NT and Λ CDM+R models. We studied many examples and found a systematic way to find the “twin Λ CDM+R model” of a given Λ CDM+NT model:

1. for any Λ CDM+NT model with a small total mass $m_0 < 0.9$ eV, the conclusion is straightforward: the Λ CDM+R model sharing the same values of N_{eff} and ω_ν has identical CMB anisotropy spectra, and a matter power spectrum differing by less than one percent on all scales. Note that the “twin Λ CDM+R model” has a different total neutrino mass than the original Λ CDM+NT one, given by the simple relation $m_0^{(R)} = q m_0^{(NT)}$.

2. for any Λ CDM+NT model with larger neutrino mass – such that the neutrinos are not ultra-relativistic at decoupling – the situation is a bit more complicated: the “twin Λ CDM+R model” does not share that same values of N_{eff} and ω_ν , because the time of equality is not strictly the same for the two models. Therefore, it is necessary to increase slightly N_{eff} and Ω_Λ in the Λ CDM+R model in order to obtain the same position and amplitude of the first peak in the CMB temperature spectrum. Finally, a simultaneous increase of N_{eff} , ω_m and n_s makes it possible to match the matter power spectra without changing the time of equality and the shape of the CMB temperature spectrum.

In both cases the differences are below the percent level for the matter power spectrum, even less for the CMB anisotropy spectra. This is too small for allowing any detection with the next generation of experiments⁹. Of course, this conclusion applies to a pure CMB and LSS analysis where all parameters are assumed to be unknown. Strong evidence for the Λ CDM+NT could still arise from external data sets: for instance, in case of contradiction (assuming standard neutrinos) between future CMB and BBN predictions for the value of N_{eff} ; or between the neutrino mass scale measured by cosmology and by beta decay experiments.

V. CONCLUSIONS

In this paper we have studied the possibility that the phase space distribution of cosmological relic neutrinos may be non-thermal, and how present observations can constrain any departure from a standard Fermi-Dirac function. The latter is expected to hold to a very good accuracy (percent level) in the standard scenario, where neutrinos last interact at the freeze out of weak interactions for temperatures of the order of MeV, and then simply free stream keeping an equilibrium distribution. However, if neutrino evolution is influenced at some later stage by some unknown and exotic phenomena, we expect that their distribution could be modified. For example, if some decoupled particle eventually decay into neutrinos in out of equilibrium conditions and after weak interaction freezing, the neutrino distribution can have large departures from a simple Fermi-Dirac function. We have investigated this model in details, for the case of light ($M \leq 1$ MeV) decoupled scalar particles decaying in neutrino/antineutrino pairs.

Neutrinos both influence the CMB spectrum and the clustering of structures on large scales. Their distribu-

⁹ This statement is easy to prove quantitatively by repeating the Fisher matrix analysis of the previous section, including an extra parameter describing the “linear deformation” of one model into another. This parameter results to be far from detectable.

tion, in fact, enters the value of the matter-radiation equality point, as well as for massive neutrinos the matter power spectrum suppression at scales smaller than the free streaming scale. The neutrino distribution can be always fully characterized by the set of its moments $Q_\alpha^{(n)}$ which in principle may all affect the cosmological evolution of perturbations. However, present data are only sensitive to the first two distribution moments. Actually, the total neutrino mass m_0 and the moment $Q_\alpha^{(1)}$ (corresponding to N_{eff}) are well constrained by the CMB and LSS data, while $Q_\alpha^{(0)}$ (corresponding to the ratio ω_ν/m_0) is not. This fact, along with the existence of a degeneracy among ω_{dm} , N_{eff} and m_0 , implies that it is presently impossible to establish whether neutrinos are thermally distributed or not, even in the most conservative scenario of no extra relativistic particles at CMB epoch apart from photons and neutrinos. In particular, in the framework of the Φ decay scenario described in Section II, the most stringent constraint on $Q_\alpha^{(0)}$ comes from BBN only, $A \leq 0.1$, rather than from CMB and LSS. The non-thermal contribution to the total neutrino energy density can then be very large or even dominant, since it is ruled by the parameter $y_* = M/(2T_D)$ which is very poorly constrained and can take very large values, $y_* \sim 10$, even for A close to the BBN upper bound.

We have also studied how these results may likely change when new data on CMB and LSS will be available. Adopting a Fisher matrix analysis we find that combining the sensitivity of the Planck experiment with the completed SDSS redshift survey, the uncertainty on the neutrino first moment N_{eff} would be reduced by almost an order of magnitude, but still the neutrino number density will be affected by a large error, see for example the results of Table II. The sensitivity to non-thermal features in the neutrino distribution highly improves only by considering a survey with the properties of a shear survey like the LSST project, and also the sensitivity of a

CMB experiment like CMBPOL. Even in this case, however, it may be quite involved to test the hypothesis of a non thermal neutrino background since, as we stressed in Section IV, a purely thermal neutrino background with extra relativistic degrees of freedom would provide an almost degenerate scenario, with the exception of predicting a different energy density at the time of primordial nucleosynthesis, and a different value for the neutrino mass scale. In the future, evidence for non-thermal distortions could possibly result from an *apparent* contradiction between the values of N_{eff} and/or m_0 probed by cosmological perturbations (assuming standard neutrinos) and those indicated respectively by primordial nucleosynthesis and particle physics experiments. In particular, an independent source of information on m_0 would greatly help. Direct neutrino mass measurements like the Tritium beta decay experiment KATRIN [49] or experiments on neutrinoless double beta decay [50], which are expected to reach a sensitivity on the neutrino mass scale of the order of $0.1 \div 0.3$ eV, combined with cosmological observations could reduce this degeneracy.

Despite of the fact that by Ockham's razor principle it is presently worth assuming a purely thermal distribution for relic neutrinos, nevertheless we think that it is remarkable that present knowledge of the $C\nu B$ features still allows for quite non standard and exotic physics which affected the evolution of the Universe at late stages. As frequently happened in the past, neutrinos can play a role in constraining such possibilities.

Acknowledgments

This research was supported by a Spanish-Italian AI, the Spanish grant BFM2002-00345, as well as CICYT-IN2P3 and CICYT-INFN agreements. SP was supported by a Ramón y Cajal contract of MEC.

-
- [1] C.L. Bennett et al., *Astrophys. J. Suppl.* **148**, 1 (2003) [astro-ph/0302207].
 - [2] G.B. Gelmini, hep-ph/0412305.
 - [3] C. Hagmann, astro-ph/9905258.
 - [4] A.D. Dolgov et al., *Nucl. Phys. B* **632**, 363 (2002) [hep-ph/0201287].
 - [5] A. Cuoco et al., *Int. J. Mod. Phys. A* **19**, 4431 (2004) [astro-ph/0307213].
 - [6] V. Barger et al., *Phys. Lett. B* **566**, 8 (2003) [hep-ph/0305075].
 - [7] A.D. Dolgov, S.H. Hansen and D.V. Semikoz, *Nucl. Phys. B* **503**, 426 (1997) [hep-ph/9703315].
 - [8] G. Mangano, G. Miele, S. Pastor and M. Peloso, *Phys. Lett. B* **534**, 8 (2002) [astro-ph/0111408].
 - [9] W. Hu, D.J. Eisenstein and M. Tegmark, *Phys. Rev. Lett.* **80**, 5255 (1998) [astro-ph/9712057].
 - [10] P. Crotty, J. Lesgourgues and S. Pastor, *Phys. Rev. D* **67**, 123005 (2003) [astro-ph/0302337].
 - [11] P. Crotty, J. Lesgourgues and S. Pastor, *Phys. Rev. D* **69**, 123007 (2004) [hep-ph/0402049].
 - [12] D.N. Spergel et al., *Astrophys. J. Suppl.* **148**, 175 (2003) [astro-ph/0302209].
 - [13] S. Hannestad, hep-ph/0412181.
 - [14] S.H. Hansen et al., *Phys. Rev. D* **65**, 023511 (2002) [astro-ph/0105385].
 - [15] G.L. Fogli et al., *Phys. Rev. D* **70**, 113003 (2004) [hep-ph/0408045].
 - [16] L. Cucurull, J.A. Grifols, and R. Toldrà, *Astropart. Phys.* **4**, 391 (1996) [astro-ph/9506040].
 - [17] A.D. Dolgov and A.Yu. Smirnov, hep-ph/0501066.
 - [18] G.F. Giudice et al., *Phys. Rev. D* **64**, 043512 (2001) [hep-ph/0012317].
 - [19] P. Adhya, D. R. Chaudhuri and S. Hannestad, *Phys. Rev. D* **68**, 083519 (2003) [astro-ph/0309135].
 - [20] S. Hannestad, *Phys. Rev. D* **70**, 043506 (2004) [astro-ph/0403291].

- [21] S. Hannestad, Phys. Rev. D **59**, 125020 (1999) [astro-ph/9903475].
- [22] M. Kaplinghat, R.E. Lopez, S. Dodelson and R.J. Scherrer, Phys. Rev. D **60**, 123508 (1999) [astro-ph/9907388].
- [23] K. Abazajian, N.F. Bell, G.M. Fuller and Y.Y. Wong, astro-ph/0410175.
- [24] A.D. Dolgov, Phys. Rept. **370**, 333 (2002) [hep-ph/0202122].
- [25] P.D. Serpico et al., JCAP **0412**, 010 (2004) [astro-ph/0408076].
- [26] R.H. Cyburt, Phys. Rev. D **70**, 023505 (2004) [astro-ph/0401091].
- [27] P.D. Serpico and G.G. Raffelt, Phys. Rev. D **70**, 043526 (2004) [astro-ph/0403417].
- [28] D. Kirkman et al., Astrophys. J. Suppl. **149**, 1 (2003) [astro-ph/0302006].
- [29] B.D. Fields and K.A. Olive, Astrophys. J. **506**, 177 (1998) [astro-ph/9803297].
- [30] Y.I. Izotov and T.X. Thuan, Astrophys. J. **602**, 200 (2004) [astro-ph/0310421].
- [31] K.A. Olive and E.D. Skillman, astro-ph/0405588.
- [32] A. Lewis and A. Challinor, Phys. Rev. D **66**, 023531 (2002) [astro-ph/0203507].
- [33] U. Seljak and M. Zaldarriaga, Astrophys. J. **469**, 437 (1996) [astro-ph/9603033].
- [34] J. Lesgourgues and S. Pastor, Phys. Rev. D **60**, 103521 (1999) [hep-ph/9904411].
- [35] S. Hannestad and G. Raffelt, JCAP **0404**, 008 (2004) [hep-ph/0312154].
- [36] A. Lewis and S. Bridle, Phys. Rev. D **66**, 103511 (2002) [astro-ph/0205436].
- [37] R. Rebolo et al., Mon. Not. Roy. Astron. Soc. **353**, 747 (2004) [astro-ph/0402466]; C. Dickinson et al., Mon. Not. Roy. Astron. Soc. **353**, 747 (2004) [astro-ph/0402498].
- [38] T.J. Pearson et al., Astrophys. J. **591**, 556 (2003) [astro-ph/0205388]; J.L. Sievers et al., Astrophys. J. **591**, 599 (2003) [astro-ph/0205387]; A.C.S. Readhead et al., Astrophys. J. **609**, 498 (2004) [astro-ph/0402359].
- [39] C. Kuo et al., Astrophys. J. **600**, 32 (2004) [astro-ph/0212289]; J.H. Goldstein et al., Astrophys. J. **599**, 773 (2003) [astro-ph/0212517].
- [40] J.A. Peacock et al., Nature **410**, 169 (2001) [astro-ph/0103143].
- [41] W.J. Percival et al., Mon. Not. Roy. Astron. Soc. **327**, 1297 (2001) [astro-ph/0105252]; Mon. Not. Roy. Astron. Soc. **337**, 1068 (2002) [astro-ph/0206256].
- [42] M. Tegmark et al., Astrophys. J. **606**, 702 (2004) [astro-ph/0310725].
- [43] A.G. Riess et al., Astrophys. J. **607**, 665 (2004) [astro-ph/0402512].
- [44] L. Verde et al., Astrophys. J. Suppl. **148**, 195 (2003) [astro-ph/0302218].
- [45] W.L. Freedman et al., Astrophys. J. **553**, 47 (2001) [astro-ph/0012376].
- [46] M. Beltrán, J. García-Bellido, J. Lesgourgues, A.R. Liddle and A. Slosar, astro-ph/0501477.
- [47] J. Lesgourgues, S. Pastor and L. Perotto, Phys. Rev. D **70**, 045016 (2004) [hep-ph/0403296].
- [48] W. Hu and T. Okamoto, Astrophys. J. **574**, 566 (2002) [astro-ph/0111606].
- [49] A. Osipowicz et al. [KATRIN Coll.], hep-ex/0109033; B. Bornschein [KATRIN Coll.], contribution to the Proceedings of AHEP 2003, Valencia (Spain), published in JHEP Proc. AHEP2003/064.
- [50] S.R. Elliott and P. Vogel, Ann. Rev. Nucl. Part. Sci. **52**, 115 (2002) [hep-ph/0202264].